ChemComm

COMMUNICATION

View Article Online
View Journal | View Issue

Cite this: *Chem. Commun.*, 2024, **60**, 91

Received 9th November 2023,
Accepted 22nd November 2023

DOI: 10.1039/d3cc05527b

rsc.li/chemcomm

Isolable rubidium and caesium derivatives of common organic carbonyl compounds†‡

Jakoba Wacker,§[ab] Jennifer R. Lynch,§[a] Sumanta Banerjee,[a] Peter A. Macdonald,[a] Alan R. Kennedy,[a] Biprajit Sarkar[b] and Robert E. Mulvey*[a]

Light alkali metal (Li, Na, K) amides have a long history of synthetic utility, but heavier (Rb, Cs) congeners have barely been studied. This study reveals remarkable structurally complex outcomes of reacting AM (HMDS) (AM = Rb, Cs; HMDS = hexamethyldisilazide) with benzaldehyde and acetophenone. Though complicated, reactions give a diversity of eye-catching isolated products, an enolate with a hexagonal prismatic network, two dienolates with distinct extended ladder motifs, and two β-imino-alkoxides comprising zig-zag chains of metal–oxygen bonds in infinite cages.

Whereas Li, Na, and K amides have long been key tools in chemists' toolbox,[1] Rb and Cs congeners have so far not merited space within it. First synthesised in 1992 by Stalke from Cs metal and free amine,[2] CsHMDS [$CsN(SiMe_3)_2$] has been the one Cs amide of note albeit featuring in only a handful of applications, though recent studies hint at a more promising future.[3–6] These include as a catalyst for selective hydrogen isotope exchange of benzylic C–H bonds with D_2;[3] as a pre-catalyst for imine to amine transfer hydrogenation,[4a] and as a mediator in magnesiate-catalysed transfer hydrogenation of alkenes to alkanes.[4b] Also reported are indirect applications where CsHMDS was either not added directly but suspected of forming *in situ*, as in catalytic alkynylations of polyfluoroarenes,[5] and in alkaline-metal-catalysed aminobenzylation of aldehydes with toluenes.[6] Since HMDS is a common Brønsted base anion[1a,7] one might intuitively expect CsHMDS to be a strong stoichiometric base, but though used to deprotonate indene and fluorene,[8] its reactivity with organic substrates has not yet been studied in any detail. While organocaesium Brønsted bases are rare, inorganic bases such as CsOH and Cs_2CO_3 have made a significant impact in organic synthesis with acidic substrates, such that a "caesium effect" has been postulated, derived from observations that these salts and their derivatives sometimes outperform smaller alkali metal congeners in assorted organic transformations. However, this is not a unified effect since it is cited in different contexts and the origin/s of this superior performance remain uncertain.[9] To gain insight into their chemistry, here we report benchmarking studies of RbHMDS and CsHMDS with the common carbonyls benzaldehyde and acetophenone, focusing on their reactivity, but tracking the remarkable structural outcomes of isolable metal products. Such structures are exceptionally rare, though a variety of crystallographically characterised monometallic and heterobimetallic CsHMDS complexes are known (Fig. 1 and Fig. S1, ESI†).[2,10]

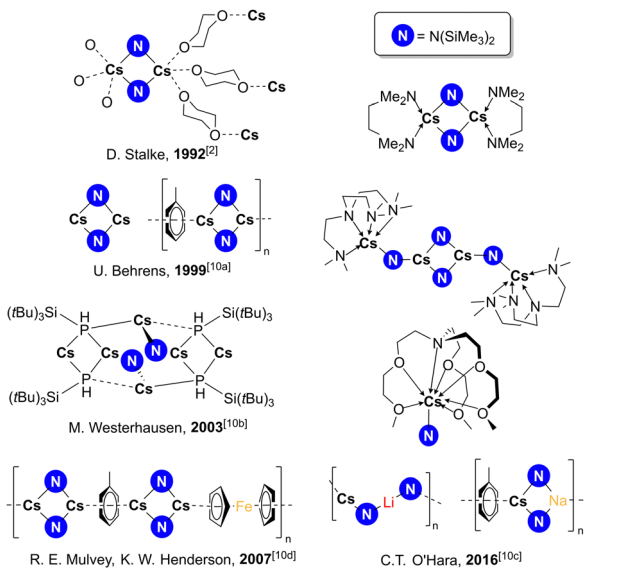

Fig. 1 Selection of crystallographically-characterised structures of $[CsN(SiMe_3)_2]$.

[a] *Department of Pure and Applied Chemistry, University of Strathclyde, Glasgow, G1 1XL, UK. E-mail: r.e.mulvey@strath.ac.uk*
[b] *Institut für Anorganische Chemie, Universität Stuttgart, Pfaffenwaldring 55, Stuttgart, 70569, Germany*

† Open data available at **https://doi.org/10.15129/5e6a35e0-1601-4b22-8bf2-2046d17b6281**.

‡ Electronic supplementary information (ESI) available. CCDC 2293054–2293058. For ESI and crystallographic data in CIF or other electronic format see DOI: **https://doi.org/10.1039/d3cc05527b**

§ JW and JRL contributed equally to this research.

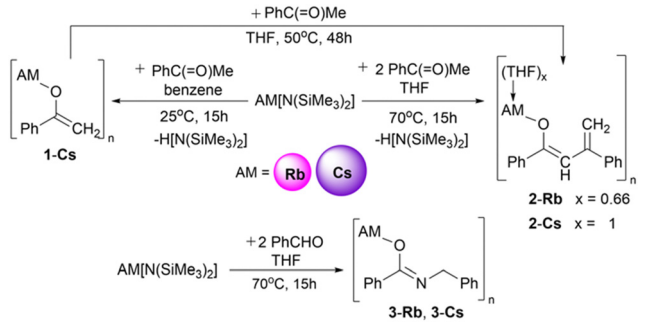

Scheme 1 Reactions of RbHMDS and CsHMDS with acetophenone and benzaldehyde in this work.

CsHMDS was mixed with acetophenone in a 1:1 ratio in benzene (Scheme 1), to form a white suspension. ^{1}H NMR analysis of the isolated solid in THF-d_8 revealed two multiplet resonances in the olefinic region at 3.28 and 3.90 ppm and aromatic signals in the range 7.02 to 7.68 ppm indicated formation of a metal-enolate species (see ESI,‡ pg. 6). The ^{13}C NMR shift of $=CH_2$ at 72.3 ppm compares to that of potassium enolate [{KOC(Mes)$=CH_2$·toluene}$_4$] (74.6 ppm, Mes = mesityl).[11] The compound's identity was confirmed by an X-ray diffraction study on crystals grown from a THF/hexane mixture at −20 °C. Enolate [CsOC(Ph)$=CH_2$]$_\infty$ (**1-Cs**) was revealed having a remarkable infinite non-covalent network with ionic Cs–O bonds in a *Pbca* space group (Fig. 2). Two asymmetric Cs-enolate bridges form a four-atom ring (grey shaded) with Cs and O atoms occupying opposite corners. The edges [2.9319(1) Å and 2.9631(6) Å] and bond angles [91.1(2)° at O and 88.8(7)° at Cs] described by this

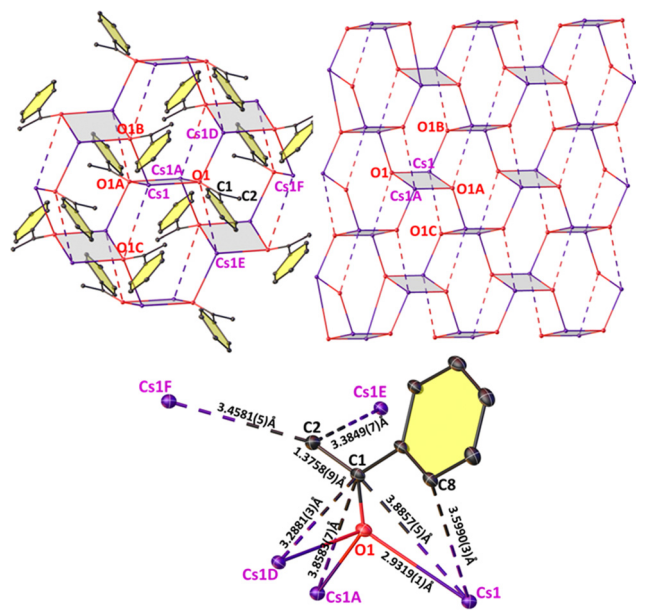

Fig. 2 (top left) Section of the infinite network structure of [CsOC(Ph)$=CH_2$]$_\infty$ (**1-Cs**); (top right); section displaying the fused distorted hexagonal Cs–O prisms. All C atoms omitted for better visualization; (bottom) section describing the interaction of five Cs atoms with one enolate anion. For clarity, thermal ellipsoids displayed at 20% probability, H atoms omitted, and aromatic rings shaded yellow.

Cs_2O_2 plane are close to that of a perfect square. These square planes stack in parallel in an alternating staggered arrangement. Four such planes from three adjacent stacks assemble together generating a distorted hexagonal prism with two parallel planes from the middle stack sharing their faces and two adjacent ones sharing one edge. These hexagonal prisms fuse together *via* all their quadrilateral faces in an infinite non-covalent network. Each Cs interacts with two other enolate O atoms [*e.g.*, Cs1–O1B, 2.9582(1) Å; Cs1–O1C 4.2610(8) Å], respectively shorter and longer than the sum of the ionic radii of [Cs (1.67 Å) and O (1.35 Å)],[12] of two adjacently stacked shaded square planes. The difference in contact lengths is the result of the shaded planes tilted at 27.0(9)° with respect to an adjacent stack. Each enolate ion engages with five Cs atoms (Fig. 2 – bottom) with O and benzylic C atoms (*e.g.*, O1 and C1) bound to three centres (Cs1, Cs1A, Cs1D); whereas terminal C2 of the enolate interacts with two Cs atoms (Cs1E, Cs1F). The C1–C2 length [1.376(11) Å] indicates a C=C double bond fitting the description of an enolate (see Table S1 for selected bond angles, ESI†). Note that this hexagonal grid network is preferred over face-on cation–π interactions between Cs and the Ph π-surface, a common feature in heavy alkali metal compounds having aryl rings.[13] Instead Cs interacts side-on to the π-electron cloud of the ring (Cs1···C8) in **1-Cs**.

While alkali metal amides, alkoxides, and enolates are known to exhibit ladder-like, cubic, or hexagonal prism motifs derived from folding of four-rung ladders,[1c,d,14] to our knowledge, the special architecture of **1-Cs** is the first such example of a Cs-organoelement compound manifested in a near hexagonal prism. Isolation of **1-Cs** therefore confirms the Brønsted basicity of CsHMDS for deprotonation of an enolizable ketone.

Mimicking the above experiment with RbHMDS led to isolation of a highly reactive set of crystals (coated in oil) which decomposed during the XRD operation. After failed attempts to obtain a clean NMR spectrum of the product, the reaction solvent was altered to more polar THF. This reaction mixture gave a white suspension that gradually converted into a dark yellow solution, which gave X-ray quality crystals at −20 °C, albeit in poor yield. Surprisingly, the structure determined (space group: *C*2/*c*) was the C–C coupled product [{RbOC(Ph)=C(H)C(Ph)$=CH_2$}$_3$·(THF)$_2$]$_\infty$ (**2-Rb**), presumably formed by a base mediated self-aldol-type reaction (Scheme S1, p12, ESI†). **2-Rb** is composed of partly solvated trinuclear asymmetric units (with disordered THF ligands) with Rb–O interactions resembling a skewed three-rung (Rb_3O_3) ladder (Fig. 3). Alternating short and long C–C bonds indicate a dienolate intermediate (see Table S2, ESI†). The planes defined by Rb_2O_2 units lie at an angle of 14.5(2)° with respect to their plane normal. Two of the three Rb atoms (Rb_2 and Rb_3) in the asymmetric unit in one disordered model are solvated by THF, whereas THF-free Rb1 has the shortest Rb_1–O_1 bond distance of 2.685(3) Å [*cf.*, Rb_2–O_2, 2.770(4) Å; Rb_3–O_3, 2.797(3) Å] due to the lower coordination. The trinuclear fused ladder propagates linearly in a slipped manner *via* interactions with Rb and the adjacent diene unit to form an infinite chain. The four sp^2 hybridized C atoms sandwich between two Rb cations or *vice versa* and lie in the range 3.131(6)–3.770(6) Å from Rb. Reaction of RbHMDS and acetophenone in 1:2 ratio in THF-d_8 reveals the appearance of a singlet C*H* resonance at 5.25 ppm of **2-Rb**

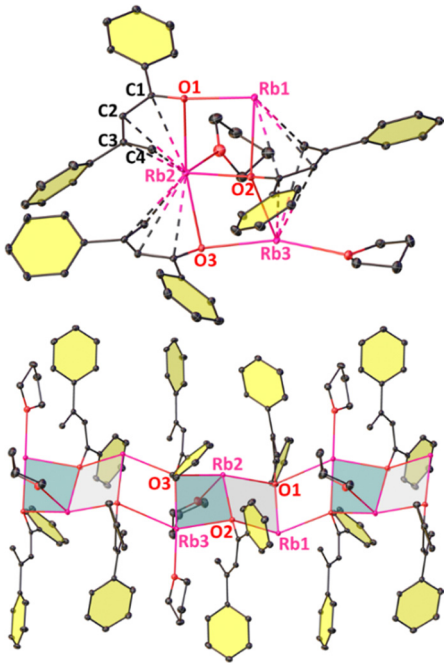

Fig. 3 (top) Asymmetric unit of the structure of [{RbOC(Ph)═C(H)C(Ph)═CH_2}$_3$·$(THF)_2$]$_\infty$ (**2-Rb**); (bottom) section of the infinite ladder of **2-Rb**. For clarity, thermal ellipsoids displayed at 20% probability, H atoms omitted, and aromatic rings shaded yellow. Rb_2O_2 rings are shaded to display the ladder's linear growth.

accompanied by doublets at 6.23 (J = 3.96 Hz) and 4.69 ppm (J = 3.80 Hz) for the terminal CH_2 H atoms in the ^{1}H NMR spectrum. Corresponding ^{13}C NMR signals appear at 90.8 ppm (for CH) and 99.5 ppm (for CH_2). Unreacted CsHMDS, acetophenone and free HMDS(H) signals can also be seen in the spectrum.

Inspired by this unexpected result, reaction of CsHMDS and acetophenone was repeated in THF to yield a similar ladder-shaped dienolate [CsOC(Ph)═C(H)C(Ph)═CH_2·THF]$_\infty$ (**2-Cs**), as confirmed by its XRD analysis ($P\bar{1}$ space group, Fig. 4). The structure of **2-Cs** bears resemblance to that of **2-Rb** as the asymmetric units [{CsOC(Ph)═C(H)C(Ph)═CH_2·THF}$_6$·THF] propagate linearly into an infinite four-rung ladder of Cs_2O_2 rings. Rungs and edges have a mean bond length of 2.899 Å and 3.209 Å, respectively. The diene π-electrons interact with Cs akin to that in **2-Rb**. ^{1}H NMR spectrum of the crystals in THF-d_8 confirmed the identity of **2-Cs** in solution through a singlet CH resonance at 5.36 ppm and doublets at 6.35 (J = 3.92 Hz) and 4.72 ppm (J = 3.20 Hz) for the terminal CH_2 atoms with aromatic signals in the range of 7.79–7.06 ppm (see ESI,‡ p. 16). Heating the CsHMDS and acetophenone mixture in THF-d_8 to 50 °C also gave **2-Cs** as evidenced by a ^{1}H NMR spectrum (see ESI,‡ p. 8).

Reports of alkali-metal dienolate structures are extraordinarily rare[15] with the one exception of Seebach's *N*,*N*′-dimethylpropyleneurea (DMPU)-solvated lithium dienolate of pinacolone, made *via* the aldol condensation product of two pinacolones. It was postulated that aldol addition occurred while making the pinacolonenolate and after a reaction sequence of water splitting to enone and deprotonation to the dienolate, the final product [(DMPU)LiOC(H)(*t*Bu)═C(H)C(*t*Bu)═CH_2]$_2$ was isolated.[15a] Since a small amount of final product was isolated, this could imply a similar pathway in forming **2-Rb/Cs**.

To test the reactivity of RbHMDS and CsHMDS in the absence of an acidic proton, stoichiometric reactions with benzaldehyde were performed in THF at 70 °C (Scheme 1). Colourless reaction mixtures turned purple for Cs and pink for Rb. Crystals grown from the supernatants at – 20 °C studied by XRD revealed them to be [RbOC(Ph)═NCH_2Ph]$_\infty$ (**3-Rb**) and [CsOC(Ph)═NCH_2Ph]$_\infty$ (**3-Cs**), which crystallised without any solvent coordination in $P2_1/c$ and $Pca2_1$ space groups respectively (Fig. S5 for **3-Rb**; Fig. 5 and Fig. S6 for **3-Cs**, ESI†). These compounds may be viewed as alkali metal β-imino-alkoxides derived from the tautomer or iminol form of *N*-(benzyl)benzamide. While the asymmetric unit of **3-Rb** contains one [RbOC(Ph)═NCH_2Ph] unit, **3-Cs** has two [CsOC(Ph)═NCH_2Ph]$_2$ units. One Cs atom in the asymmetric unit bridges two β-imino-alkoxide anions *via* their O atoms while the other Cs binds *via* the N atom and the π-cloud of Ph ring closest to N (Cs···C_t, 3.359 Å, C_t = centroid of Ph ring) of one anion. Analysing bond metrics of **3-Rb** and **3-Cs** revealed the existence of Rb/Cs–O σ-interactions [Rb1–O1, 2.877(9) Å; Cs1–O1, 2.9233(5) Å, Cs1–O2, 2.9837(3) Å] and of an unsaturated N environment [for **3-Rb**

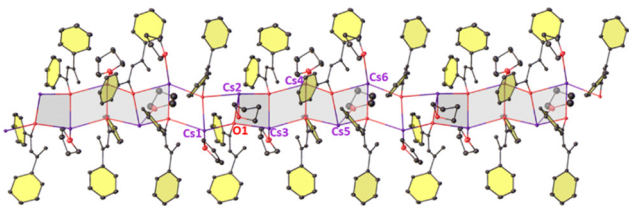

Fig. 4 Section of the infinite ladder structure of [CsOC(Ph)═C(H)C(Ph)═CH_2·THF]$_\infty$ (**2-Cs**). For clarity, thermal ellipsoids at 20% probability, H atoms omitted, and aromatic rings shaded yellow. Cs_2O_2 rings are shaded to display the extended linear growth. The uncoordinated THF molecule in the crystal lattice has been removed for clarity.

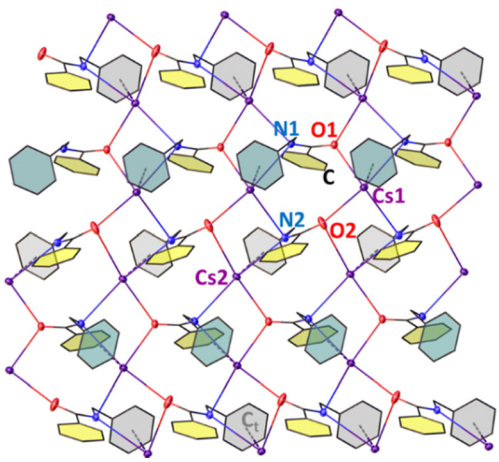

Fig. 5 Section of the network structure of [CsOC(Ph)═NCH_2Ph]$_\infty$ (**3-Cs**). Thermal ellipsoids of all non-C/H atoms displayed at 25% probability, and C atoms reduced to 5% for clarity. H atoms omitted, and aromatic rings shaded in yellow, grey, and teal for clear depiction of M···π interactions. C_t depicts centroid of Ph rings.

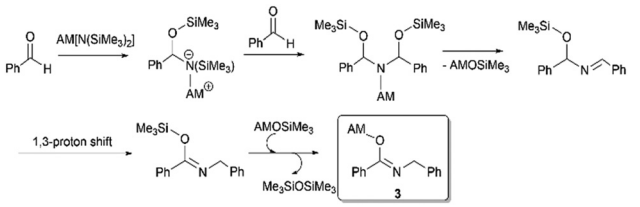

Scheme 2 General scheme representing possible mechanism of formation of **3**.

C1═N1 1.3152(9) Å; for **3-Cs** C1═N1 1.2833(7) Å, C16═N2 1.303(1) Å] (see Tables S4 and S5, ESI†).

3-Rb forms a cage-like network comprising parallel zig-zag Rb–O–Rb chains which are intercalated by Rb–N and Rb–π (η^6 to the Ph ring shaded grey, η^2 to the C═N bond, and η^1 to the *ipso* C of the Ph ring shaded yellow) interactions from neighbouring β-imino-alkoxide moieties. Rb coordinates to two O and N atoms forming two different cyclic rings, a Rb–O–Rb–N 4-atom and a highly distorted Rb–O–C–N–Rb–O–C–N 8-atom ring. Each former ring is fused with the latter rings on all sides. This allows the 4-atom grids to propagate linearly in one direction (vertically in Fig. S5, ESI†), *via* the Rb corners giving it a unique cage shape. The cage motif is preserved in **3-Cs** with interlocking zig-zag Cs–O–Cs chains containing an excess of Cs–π interactions on account of the larger radius of Cs *versus* Rb. Interestingly, this is a marked deviation from the usual aza-Peterson olefination mechanism with NaHMDS and benzaldehyde affording *N*-(trimethylsilyl)imine, an intermediate in the reaction pathway for aminobenzylation of aldehyde with NaHMDS/caesium trifluoroacetate co-operation.[6a] Though the mechanism of formation of **3** is unknown, germane literature by Toru *et al*.[16] reported heating 4-pyridinecarboxaldehyde and HMDS(H) in a 2 : 1 ratio at 70 °C to afford *N*-(pyridin-4-ylmethyl)isonicotinamide. Reaction steps involve breaking a Si–N bond, forming a strong Si–O bond, then condensation to the imine which tautomerizes to the amide *via* a 1,3-proton shift. We have postulated a mechanism for formation of **3** (Scheme 2) along similar lines.

In conclusion, this study reveals that both CsHMDS and RbHMDS display interesting reactivities with organic carbonyl substrates. With acetophenone, CsHMDS behaves predictably as a Brønsted base deprotonating the α-CH_3 group, but the reaction is still novel through the remarkable hexagonal prism shaped network of the enolate product (**1-Cs**). Adding more novelty, in donor THF, the alkali metal enolates formed *in situ* ultimately produces dienolates **2-Rb** and **2-Cs**, which have rarely been isolated for any alkali metal. Further diversity is seen with benzaldehyde in producing β-imino-alkoxides **3-Rb** and **3-Cs**, which both adopt eye-catching cage networks that interconnect zig-zag M–O–M chains but in distinct ways. Finally, while this study shows that RbHMDS and CsHMDS can exhibit Brønsted basicity, some reactions and all the new structures have unique features that demand these heavier alkali metal amides should be studied with a much wider range of organic substrates.

This research was supported by the Leverhulme Trust (grant award no: RPG-2019-264).

Conflicts of interest

The authors have no conflicts of interest to declare.

Notes and references

1 (*a*) M. Lappert, P. Power, A. Protchenko and A. Seeber, *Metal Amide Chemistry*, Wiley, Chichester, 2009, pp. 7–38; (*b*) P. C. Andrews, K. W. Henderson and K. Ruhlandt-Senge, *Comprehensive organometallic chemistry III*, ed. R. H. Crabtree and D. M. P. Mingos, Elsevier, Oxford, 2006, pp. 1–66; (*c*) R. E. Mulvey, *Chem. Soc. Rev.*, 1991, **20**, 167–209; (*d*) R. E. Mulvey, *Chem. Soc. Rev.*, 1998, **27**, 339–346; (*e*) S. D. Robertson, M. Uzelac and R. E. Mulvey, *Chem. Rev.*, 2019, **119**, 8332–8405; (*f*) T. X. Gentner and R. E. Mulvey, *Angew. Chem., Int. Ed.*, 2021, **60**, 9247–9262.
2 F. T. Edelmann, F. Pauer, M. Wedler and D. Stalke, *Inorg. Chem.*, 1992, **31**, 4143–4146.
3 H.-Z. Du, J.-Z. Fan, Z.-Z. Wang, N. A. Strotman, H. Yang and B.-T. Guan, *Angew. Chem., Int. Ed.*, 2023, **62**, e202214461.
4 (*a*) P. A. Macdonald, S. Banerjee, A. R. Kennedy, A. van Teijlingen, S. D. Robertson, T. Tuttle and R. E. Mulvey, *Angew. Chem., Int. Ed.*, 2023, **62**, e202304966; (*b*) T. X. Gentner, A. R. Kennedy, E. Hevia and R. E. Mulvey, *ChemCatChem*, 2021, **13**, 2371–2378.
5 M. Shigeno, T. Okawa, M. Imamatsu, K. Nozawa-Kumada and Y. Kondo, *Chem. – Eur. J.*, 2019, **25**, 10294–10297.
6 (*a*) Z. Wang, Z. Zheng, X. Xu, J. Mao and P. J. Walsh, *Nat. Commun.*, 2018, **9**, 3365; (*b*) Y. Gu, Z. Zhang, Y.-E. Wang, Z. Dai, Y. Yuan, D. Xiong, J. Li, P. J. Walsh and J. Mao, *J. Org. Chem.*, 2022, **87**, 406–418.
7 (*a*) R. E. Mulvey and S. D. Robertson, *Angew. Chem., Int. Ed.*, 2013, **52**, 11470–11487; (*b*) R. A. Woltornist and D. B. Collum, *J. Am. Chem. Soc.*, 2021, **143**, 17452–17464; (*c*) M. P. Coles, *Coord. Chem. Rev.*, 2015, **297–298**, 2–23.
8 S. Neander, U. Behrens and F. Olbrich, *J. Organomet. Chem.*, 2000, **604**, 59–67.
9 (*a*) H. Chen, W. Dai, Y. Chen, Q. Xu, J. Chen, L. Yu, Y. Zhao, M. Yea and Y. Pan, *Green Chem.*, 2014, **16**, 2136–2141; (*b*) R. Rabie, M. M. Hammouda and K. M. Elattar, *Res. Chem. Intermed.*, 2017, **43**, 1979–2015.
10 (*a*) S. Neander and U. Behrens, *Z. Anorg. Allg. Chem.*, 1999, **625**, 1429–1434; (*b*) M. Westerhausen, S. Weinrich, B. Schmid, S. Schneiderbauer, M. Suter, H. Nöth and H. Piotrowski, *Z. Anorg. Allg. Chem.*, 2003, **629**, 625–633; (*c*) A. I. Ojeda-Amador, A. J. Martínez-Martínez, A. R. Kennedy and C. T. O'Hara, *Inorg. Chem.*, 2016, **55**, 5719–5728; (*d*) J. J. Morris, B. C. Noll, G. W. Honeyman, C. T. O'Hara, A. R. Kennedy, R. E. Mulvey and K. W. Henderson, *Chem. – Eur. J.*, 2007, **13**, 4418–4432.
11 X. He, B. C. Noll, A. Beatty, R. E. Mulvey and K. W. Henderson, *J. Am. Chem. Soc.*, 2004, **126**, 7444–7445.
12 (*a*) L. H. Ahrens, *Geochim. Cosmochim. Acta*, 1952, **2**, 155–169; (*b*) Database of Ionic Radii, **https://abulafia.mt.ic.ac.uk/shannon/ptable.php**, (accessed July 2023).
13 (*a*) M. G. Davidson, D. Garcia-Vivo, A. R. Kennedy, R. E. Mulvey and S. D. Robertson, *Chem. – Eur. J.*, 2011, **17**, 3364–3369; (*b*) A. Rae, K. M. Byrne, S. A. Brown, A. R. Kennedy, T. Krämer, R. E. Mulvey and S. D. Robertson, *Chem. – Eur. J.*, 2022, **28**, e202104260.
14 (*a*) J. R. Lynch, A. R. Kennedy, J. Barker, J. Reid and R. E. Mulvey, *Helv. Chim. Acta*, 2022, **105**, e202200082; (*b*) P. A. Macdonald, S. Banerjee, A. R. Kennedy, R. E. Mulvey and S. D. Robertson, *Polyhedron*, 2023, **234**, 116302.
15 (*a*) R. Amstutz, J. D. Dunitz, T. Laube, W. B. Schweizer and D. Seebach, *Chem. Ber.*, 1986, **119**, 434–443; (*b*) M. Oiarbide and C. Palomo, *Chem. – Eur. J.*, 2021, **27**, 10226–10246; (*c*) T. Murahashi and H. Kurosawa, *J. Organomet. Chem.*, 1999, **574**, 142–147.
16 H. Uchida, T. Shimizu, P. Y. Reddy, S. Nakamura and T. Toru, *Synthesis*, 2003, 1236–1240.

